# Investigation of equilibrium and kinetics of Cr(VI) adsorption by dried *Bacillus cereus* using response surface methodology

Kai Yang, Jing Zhang, Tao Yang and Hongyu Wang

## ABSTRACT

In this study, response surface methodology (RSM) based on three-variable-five-level central composite rotatable design was used to analyze the effects of combined and individual operating parameters (biomass dose, initial concentration of Cr(VI) and pH) on the Cr(VI) adsorption capacity of dried *Bacillus cereus*. A quadratic polynomial equation was obtained to predict the adsorbed Cr(VI) amount. Analysis of variance showed that the effect of biomass dose was the key factor in the removal of Cr(VI). The maximum adsorbed Cr(VI) amount (30.93 mg g$^{-1}$) was found at 165.30 mg L$^{-1}$, 2.96, and 3.01 g L$^{-1}$ for initial Cr(VI) concentration, pH, and biosorbent dosage, respectively. The surface chemical functional groups and microstructure of unloaded and Cr(VI)-loaded dried *Bacillus cereus* were identified by Fourier transform infrared spectroscopy (FTIR) and scanning electron microscopy (SEM), respectively. Besides, the results gained from these studies indicated that Langmuir isotherm and the second-order rate expression were suitable for the removal of Cr(VI) from wastewater. The results revealed RSM was an effective method for optimizing biosorption process, and dried *Bacillus cereu*s had a remarkable performance on the removal of Cr(VI) from wastewater.

**Key words** | *Bacillus cereus*, biosorption, central composite rotable design, Cr(VI), response surface methodology

**Kai Yang** (corresponding author)
**Jing Zhang**
**Tao Yang**
**Hongyu Wang**
School of Civil Engineering,
Wuhan University,
Wuhan 430072,
China
E-mail: yk220220@126.com

## INTRODUCTION

The release of large quantities of heavy metals from industries into the environment is posing serious risks to human health and environment (Saraswat & Raj 2010; Flouty & Estephane 2012; Li *et al.* 2013). Chromium, which is extensively used in electroplating, steel production, wood preservation and leather tanning, is a very common pollutant in industrial effluents, and has become an environmental problem around the world (Das 2010). Due to its non-biodegradability, toxicity, mobility in natural water ecosystems and bioaccumulation in living tissues, the concentration of chromium ion in the solution exceeding its critical level has an adverse impact on the environment and public health (Rubio *et al.* 2002; Ngah & Hanafiah 2008; Landaburu-Aguirre *et al.* 2010; Choppala *et al.* 2013). Besides, the discharge standards of heavy metals approved by national or international agencies become more and more stringent. All those reasons have accelerated the search for a cost-effective and environment friendly method for the removal of chromium to an environmentally safe level.

The conventional methods, such as chemical precipitation, solvent extraction, coagulation–flocculation, photocatalysis, flotation, membrane separation and adsorption, are used to remove metal ions from wastewaters and effluents (Demirbas 2008; Wang & Chen 2009; Suazo-Madrid *et al.* 2011). However, due to the feasibility of economical and technical factors, and the avoidance of chemical sludge, the implementation of these methods is limited (Al-Rub *et al.* 2006). Biosorption, which uses biomass or natural substances as a sorbent to remove the toxic heavy metals from wastewater, has been considered as an attractive alternative to the traditional methods (Demirbas 2008). The mechanisms of biosorption are based on physico-chemical interactions between metal and functional groups of the cell wall (Çelekli &Bozkurt 2011). Biological biomasses, such as bacteria, yeast, fungi, and algae, have been used for their biosorptive potential (Çelekli & Bozkurt 2011). Numerous studies have reported that due to its easy handling, no nutrient requirements, low costs and no effect from the toxicity of the

metal ions, the use of nonliving biomass is more convenient and practical than that of living biomass. Besides, many studies have shown that biosorption of metal ions by biosorbents is strongly dependent upon the initial concentration of metal ions and adsorption conditions (Al-Rub *et al.* 2006; Demirbas 2008). Hence, an effective method to assess the effect (single effect and interactive effects) of variables on the removal of heavy metals is very important. The traditional methods used to assess the influence of factors usually change one independent variable parameter, while maintaining all others at a constant level. However, because of the extra chemical consumption, excessive time and human power requirements, the traditional methods are not valid. Response surface methodology (RSM) design is a collection of statistical and mathematical techniques, which are useful for designing experiments, building models, and analyzing the effects of several independent variables on the response design and optimization process (Amini *et al.* 2008, 2009). The main advantage of RSM is the decreased number of experimental trials required to interpret multiple parameters and their interactions. In order to determine a suitable polynomial equation for describing the response surface, RSM can be employed to optimize the process.

Nevertheless, few studies have been found in the literature for optimization of adsorption of Cr(VI) ions by dried *Bacillus cereus*. Therefore, in this research, the objective was to optimize the adsorption conditions of Cr(VI) ions by dried *Bacillus cereus* using RSM. The effects of variables including biomass dose, initial concentration of Cr(VI) ions and initial pH were investigated by three-variable-three-level central composite design (CCD). This process was analyzed using Matlab in RSM. An empirical model correlating response to the three variables was then developed. The biosorbent was characterized through Fourier transform infrared (FTIR: Nicolet 5700 spectrometer, USA) and scanning electron microscope (SEM: Quanta 200, FEI, China) to know the physico-chemical properties of the biosorbent. In this work, we also applied common methods that employ various kinetics models and isotherm parameters calculation to determine the adsorption capacity.

## MATERIALS AND METHODS

### Preparation of adsorbent

*Bacillus cereus* individuals were isolated from the sediment from a sequencing batch reactor. The isolated bacteria were cryopreserved in solid medium at 4 °C. At the beginning of the experiment, the bacteria were transferred to a 500 mL conical flask containing 300 mL broth medium (1.2 g beef extract, 4.0 g peptone and 2.0 g NaCl), and shaken at 150 rpm and 30 °C for 36 h, then harvested by centrifugation at 9,000 rpm and 4 °C for 6 min. The precipitate was washed with distilled water, dried at 60 °C for 12 h then ground and sieved into different fractions. The 0.56- to 0.85-mm particle size fraction was used in the experiments.

### Cr(VI) solution standards

The Cr(VI) ion solution was prepared from potassium dichromate ($K_2Cr_2O_7$). Standard stock solutions were prepared in distilled water, slightly acidified with 1 N HCl and 1N NaOH, and sterilized at 121 °C for 15 min, then kept at 28 °C. The glassware was leached in 3 N HCl and rinsed several times with distilled water before use to avoid metal contamination.

### Analysis and measurements

The concentrations of residual Cr(VI) ions in the supernatant solutions were determined using UV-VIS spectrophotometry (SP-1920, China). The metal uptake yield from the liquid phase was determined at the beginning $c_i$ (mg L$^{-1}$) and at the end $c_f$ (mg L$^{-1}$). The following equation was used to compute biosorbent uptake yield (mg g$^{-1}$), where $v$ is the volume of the solution (mL) and $w$ is the mass of the biosorbent (g) (Şahan & Öztürk 2014)

$$q = (c_i - c_f) \times \frac{v}{1000\,w} \tag{1}$$

### Experimental design

The optimum condition for the adsorption of Cr(VI) by dried *Bacillus cereus* was determined by RSM. RSM is a statistical technique used for multiple regression analysis of quantitative data obtained from statistically designed experiments by solving the multivariable equations simultaneously (Amini *et al.* 2008). Due to its suitability to fit a quadratic surface, which usually works well for process optimization, CCD is most frequently used for RSM design. The adsorbed Cr(VI) amount was statistically modeled and designed by RSM, and CCD was used to optimize the biosorption process.

This design consists of full factorial or fractional factorial design to determine effects of variables and interactions, an additional design, often a star design in which experimental points are at a $\alpha$ distance from its center which can be used to determine quadratic terms and central point to determine curvature of response. A central composite

rotable design (CCRD) for three factors was employed for this experimental design to provide data to model the effects of the independent variables, such as pH, biomass concentration (g L$^{-1}$) and initial lead concentration (mg L$^{-1}$), and the three-variable-five-level design as shown in Table 1 was used for the optimization procedure. The second-order quadratic equation to predict the maximum adsorbed Cr(VI) amount is given below:

$$Y = \beta_0 + \sum_{i=1}^{k} \beta_i X_i + \sum_{i=1}^{k} \beta_{ii} X_i^2 + \sum \sum_{i<j=1}^{k} \beta_{ij} X_i X_j = e \qquad (2)$$

where $Y$ is the predicted response, $X_i, X_j, ..., X_k$ are the input variables, which affect the response $Y$, $X_i^2$ $X_j^2, ..., X_k^2$ are the square effects, $X_i X_j$ and $X_j X_k$ are the interaction effects, $\beta_0$ is the intercept term, $b_i$ (i = 1, 2,..., k) is the linear effect, $b_{ii}$ (i = 1, 2, ..., k) is the squared effect, $b_{ij}$ (i = 1, 2, ..., k; j = 1, 2, ..., k) is the interaction effect and e is a random error (Şahan & Öztürk 2014; Turkyilmaz *et al.* 2014).

The analysis of variance (ANOVA) data were computed by Matlab in order to obtain the interaction between the processed variables and the response. The quality of the fit of the polynomial model was expressed by the coefficient of determination ($R^2$) and the statistical significance was checked by the F test using the same program.

## Adsorption kinetics and isotherms

Adsorption kinetics were determined in the following experiment: 3.01 g L$^{-1}$ of adsorbent mass and 50 mL of aqueous Cr(VI) solution with initial concentration in the range from 50 to 150 mg L$^{-1}$ were added to a 250 mL flask and incubated in a water bath set to room temperature (28 °C), with shaking at pH 2.9 and the speed of 150 rpm for 60 min.

Various adsorption kinetic models have been used to investigate the controlling mechanism of the adsorption process. The adsorption data were analyzed using first- and second-order kinetic models, which are shown in linear form by the following equations, respectively (Buntić *et al.* 2013):

$$\log(q_e - q_t) = \log q_e - \frac{k_1}{2.303} t \qquad (3)$$

$$\frac{t}{q_t} = \frac{1}{k_2 q_e{}^2} + \frac{1}{q_t} t \qquad (4)$$

where $q_t$ and $q_e$ (mg g$^{-1}$) are the amounts of the metal ions adsorbed at $t$ (min) and equilibrium, respectively, and $k_1$ (1/min) and $k_2$ (g/mg min) are the rate constants of the pseudo-first-order and second-order, respectively.

Isotherm studies were performed by preparing Cr(VI) solutions with the initial concentration of Cr(VI) solution in the range from 50 to 150 mg L$^{-1}$, and mixing the solutions with 3.01 g L$^{-1}$ g of the adsorbent followed by agitating the mixture (150 rpm, at 28 °C) at pH 2.9 until equilibrium. In this study, the most common adsorption isotherm equations, including Langmuir and Freundlich, were tested to understand the nature of the adsorption mechanism.

The Langmuir isotherm theory assumes monolayer coverage of adsorbate over a homogeneous adsorbent surface (Güzel *et al.* 2015). The linearized Langmuir isotherm equation is represented by Equation (5):

$$\frac{c_e}{q_e} = \frac{1}{b q_m} + \frac{c_e}{q_m} \qquad (5)$$

where $q_e$ (mg g$^{-1}$) is the adsorbed Cr(II) amount at equilibrium, $c_e$ (mg L$^{-1}$) is the supernatant concentration at equilibrium, and $q_m$ (mg g$^{-1}$) and $b$ (L mg$^{-1}$) are constants representing the maximum adsorption capacity and the Langmuir constant related to the heat of adsorption, respectively.

The Freundlich isotherm is an empirical equation based on sorption on a heterogeneous surface or surface supporting sites of varied affinities (Güzel *et al.* 2015). The linear form of the Freundlich isotherm is given by the following equation:

$$\ln q_e = \ln K_e + \frac{1}{n} \ln C_e \qquad (6)$$

**Table 1** │ Independent variables and levels used for CCRD in Cr(VI) biosorption process

| Variables | Symbols | Levels | | | | |
|---|---|---|---|---|---|---|
| | | −1.682 (-α) | −1 | 0 | 1 | 1.682 (α) |
| pH | X$_1$ | 1.00 | 1.88 | 3.00 | 4.12 | 5.00 |
| Biomass concentration (g L$^{-1}$) | X$_2$ | 2.40 | 2.65 | 3.00 | 3.36 | 3.60 |
| Initial Ni$^{2+}$ concentration (mg L$^{-1}$) | X$_3$ | 100.00 | 120.27 | 150.00 | 179.73 | 200.00 |

where $K_e$ and $n$ are the Freundlich constants characteristic of the system.

Langmuir isotherm can be expressed in terms of a dimensionless separation factor, $R_L$, which describes the type of isotherm:

$$R_L = \frac{1}{1 + bC_0} \tag{7}$$

where $C_0$ is the initial concentration of Cr(VI). The magnitude of $R_L$ determines the feasibility of the adsorption process. If $R_L > 1$, adsorption is unfavorable; if $R_L = 1$, adsorption is linear; if $R_L < 1$, adsorption is favorable and if $R_L = 0$, adsorption is irreversible (Sarkar & Santra 2015).

## Characterization of the biosorbent

Characterization of biosorbent surface and structure hold keys to understand the metal binding mechanism onto biomass. In this study, the infrared spectrum of raw and metal laden adsorbents was obtained by the use of a FTIR spectrometer (Perkin–Elmer Spectrum 100 FTIR Spectrometer) equipped with an Attenuated Total Reflection accessory (Perkin Elmer) to identify the functional groups responsible for the sorption. SEM was used to show the morphology of the dried *Bacillus cereus* biomass. The samples were dried by liquefied nitrogen, coated with gold and observed with a microscope. Finally, images of the samples were taken under SEM.

## RESULTS AND DISCUSSION

### Experimental design

Experimental design of CCRD with the corresponding results and the adsorbed Cr(VI) amount (experimental and predicted) for the process response are presented in Table 2. The second-order equation for the estimation of the adsorbed Cr(VI) amount in terms of pH ($X_1$), biosorbent dosage ($X_2$) and initial concentration of Cr(VI) ($X_3$) was

**Table 2** | CCRD arrangement and responses for biosorption process

| Run | Point type | Factors | | | Adsorbed amount of Cr ion (mg L$^{-1}$) | Cr(VI) ion removal (mg g$^{-1}$) | |
| | | $X_1$ | $X_2$ | $X_3$ | | Experimental | Predicted |
|---|---|---|---|---|---|---|---|
| 1 | Fact | 1.88 | 2.64 | 120.27 | 27.37 | 10.37 | 11.93 |
| 2 | Fact | 1.88 | 3.36 | 179.73 | 95.74 | 28.49 | 27.96 |
| 3 | Fact | 4.12 | 3.36 | 179.73 | 89.38 | 26.60 | 25.54 |
| 4 | Fact | 4.12 | 3.36 | 120.27 | 45.19 | 13.45 | 15.18 |
| 5 | Fact | 1.88 | 3.36 | 120.27 | 43.91 | 13.07 | 15.35 |
| 6 | Fact | 4.12 | 2.64 | 120.27 | 36.28 | 13.74 | 14.78 |
| 7 | Fact | 1.88 | 2.64 | 179.73 | 79.20 | 30.00 | 28.61 |
| 8 | Fact | 4.12 | 2.64 | 179.73 | 80.47 | 30.48 | 28.88 |
| 9 | Axial | 3.00 | 3.00 | 200.00 | 79.10 | 26.37 | 29.34 |
| 10 | Axial | 3.00 | 2.40 | 150.00 | 54.56 | 22.73 | 23.21 |
| 11 | Axial | 3.00 | 3.00 | 100.00 | 31.28 | 10.43 | 6.74 |
| 12 | Axial | 1.00 | 3.00 | 150.00 | 69.83 | 23.28 | 22.55 |
| 13 | Axial | 3.00 | 3.60 | 150.00 | 87.64 | 24.35 | 23.14 |
| 14 | Axial | 5.00 | 3.00 | 150.00 | 68.55 | 22.85 | 22.94 |
| 15 | Center | 3.00 | 3.00 | 150.00 | 91.46 | 30.49 | 30.39 |
| 16 | Center | 3.00 | 3.00 | 150.00 | 90.19 | 30.06 | 30.39 |
| 17 | Center | 3.00 | 3.00 | 150.00 | 94.01 | 31.34 | 30.39 |
| 18 | Center | 3.00 | 3.00 | 150.00 | 88.92 | 29.64 | 30.39 |

represented in terms of coded factors ($-\alpha$, $-1, 0$ and $+1$, $+\alpha$) as follows:

Adsorbed Cr(VI) amount (mg g−1) $Y$

$$= -377.2206 + 19.4754\,X_1 + 138.9367\,X_2$$
$$+ 2.0399\,X_3 - 1.6652\,X_1 X_2 - 0.0194\,X_2 X_3$$
$$- 0.0910\,X_2 X_3 - 1.9122\,X_1^2 - 20.0578\,X_2^2$$
$$- 0.0049\,X_3^2 \tag{8}$$

Equation (8) represents the quantitative effect of the process variables ($X_1$, $X_2$, and $X_3$) and their interactive effects on the response ($Y$). A positive sign in the equation represents a synergistic effect of the variables, while a negative sign indicates an antagonistic effect of the variables. The results of the ANOVA for the proposed statistical model and their model coefficients are given in Tables 3 and 4, respectively.

The $F$ value, which is a ratio of the mean square due to regression to the mean square due to error, was converted

**Table 3** │ Regression coefficients of predicted quadratic polynomial model for adsorbed Cr(VI) amount

| Terms | Regression coefficients |
|---|---|
| Intercepts | |
| $\beta_0$ | −377.2206 |
| Linear term | |
| $\beta_1$ | 19.4754 |
| $\beta_2$ | 138.9367 |
| $\beta_3$ | 2.0399 |
| Quadratic | |
| $\beta_{11}$ | −1.6652 |
| $\beta_{22}$ | −0.0194 |
| $\beta_{33}$ | −0.0910 |
| Interaction | |
| $\beta_{12}$ | −1.9122 |
| $\beta_{13}$ | −20.0578 |
| $\beta_{23}$ | −0.0049 |

into its corresponding $P$ value. From a statistical point of view, if the $P$ value $< 0.05$, then the model is statistically significant. As the $P$ value decreases, it becomes less likely that the effect is due to chance, and more likely that there was a real cause. In this case, the $P$ value of model was 0.00001 and it was significant. Besides, $R^2 = 0.955$ for Equation (2) indicated a good fitting for the experimental data and predicted values.

A plot of observed removal of Cr(VI) versus those obtained from Equation (7) is shown in Figure 1. The figure proves that the predicted response from the empirical model was in good agreement with the observed data.

## Effect of process variables

To gain better understanding of the effects of the three independent variables and their interactions on the Cr(VI) amount adsorbed by dried *Bacillus cereus*, three-dimensional response surface plots were constructed based on the quadratic model. Figure 2 shows the results of fitting experimental Cr(VI) adsorption data to the response model represented by Equation (7).

Figure 2(a)–(c) are drawn at constant values of 150 mg L$^{-1}$ initial Cr(VI) concentration ($X_3$), 3 g L$^{-1}$ biomass concentration ($X_2$) and pH ($X_1$) = 3, respectively. Figure 2(a)–(c) show the simultaneous effects of pH and biosorbent dosage, the simultaneous effects of pH and initial Cr(VI) concentration, and the simultaneous effects of biosorbent dosage and initial Cr(VI) concentration on the adsorbed Cr(VI) amount, respectively.

## Effect of biosorbent dosage

The effect of biosorbent dosage was found to be the most significant among the studied variables on the adsorbed Cr(VI) amount. Figure 2(a) and (c) show the combined effect of biosorbent dosage with pH and the initial concentration of Cr(VI) on the adsorbed Cr(VI) amount. According to Figure 2(a) and (c), the adsorbed Cr(VI) amount was highly dependent on the increase in biosorbent dosage; the
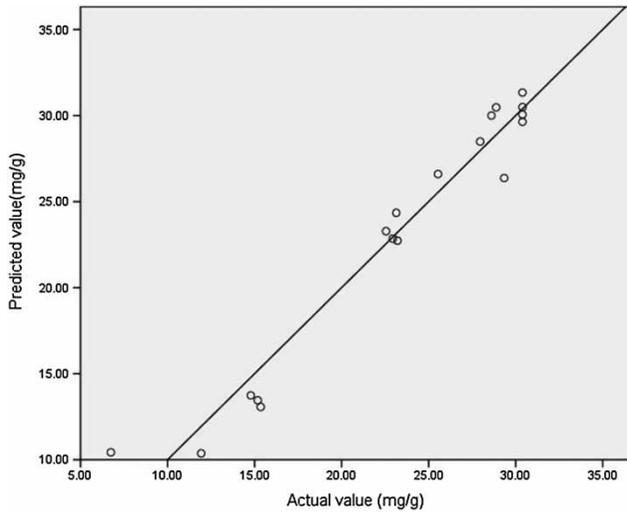
**Table 4** │ ANOVA for adsorbed Cr(VI) amount model

| | Sum of squares | df | Mean square | F value | P value | $R^2$ | |
|---|---|---|---|---|---|---|---|
| Model | 929.433 | 1 | 929.433 | 339.059 | 0.000 | 0.955 | Significant |
| Residual | 43.859 | 16 | 2.741 | | | | |
| Lack-of-fit | 42.276 | 3 | 3.252 | 6.160 | 0.180 | | |
| Pure error | 1.583 | 13 | 0.528 | | | | |
| Total | 433.942 | 17 | | | | | |

**Figure 1** │ The observed Cr(VI) uptake versus predicted Cr(VI) uptake capacity of adsorbent.

maximum biosorption (30.93 mg g$^{-1}$) was obtained when the biosorbent dosage was 3.01 g L$^{-1}$. Biosorption of Cr(VI) is proportional to the binding sites. A higher dose of biosorbent in the solution leads to greater availability of

exchangeable sites for the ions, so the adsorbed Cr(VI) amount increased with increasing biosorbent dosage. However, the adsorbed Cr(VI) amount decreased when biomass dosage was above 3.01 g L$^{-1}$. This behavior was attributed to a partial aggregation of biomass, which reduced availability of exchangeable sites for the biosorption (Ibrahim 2011).

## Effect of pH

The pH of the medium affects the solubility of metals and the ionization state of functional groups present in the biosorbent (Subbaiah & Yun 2013). Figure 2(a) and (b) show the interactive effect of pH with biosorbent dosage and initial concentration of Cr(VI) on the adsorbed Cr(VI) amount. It can be seen from the response graphs that the adsorption capacity of Cr(VI) increased as the pH increased, reached a maximum (30.93 mg g$^{-1}$) at pH 2.96, then decreased as the pH continued increasing. The lower adsorbed amount was apparent at low pH, which could be attributed to the presence of a higher concentration of H$^+$ in the solution, which could
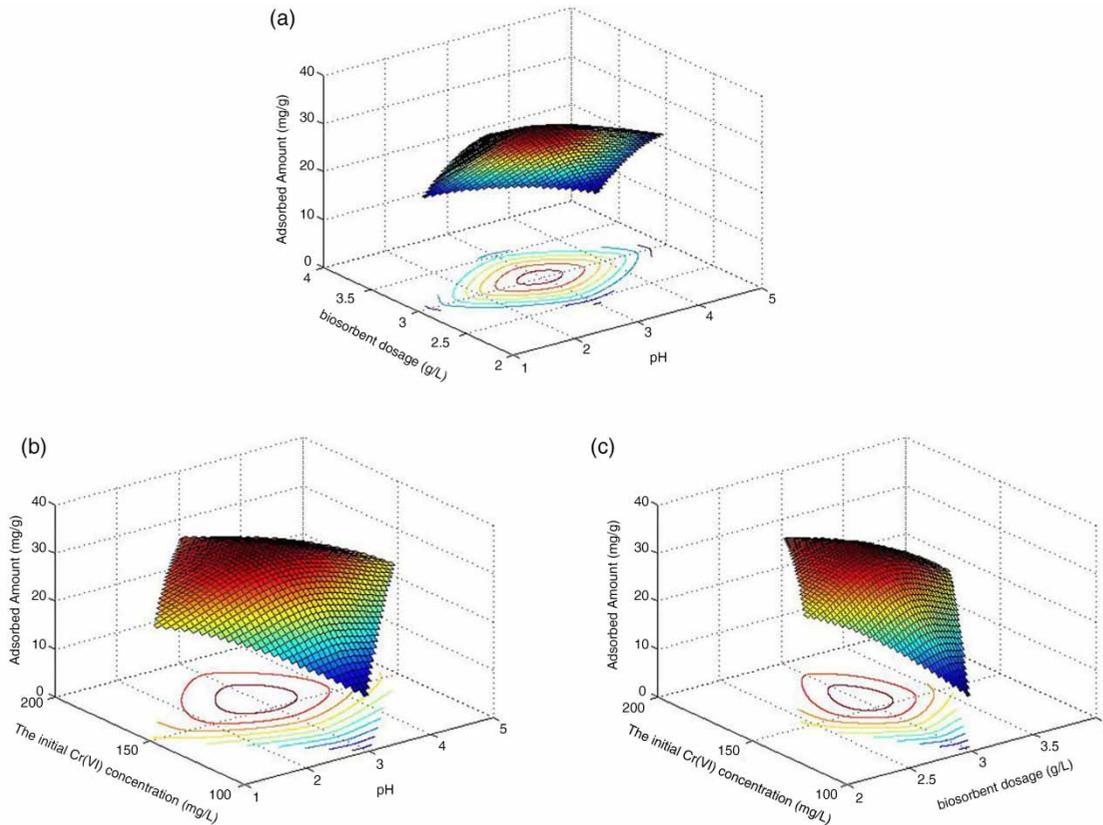


**Figure 2** │ Response surfaces for combined effect of: (a) pH and biosorbent dosage at constant initial Cr(VI) concentration of 150 mg L$^{-1}$; (b) pH and initial Cr(VI) concentration at constant biosorbent dosage 3 mg g$^{-1}$; and biosorbent dosage and initial Cr(VI) concentration at constant pH of 3.0; on the amount of Cr(VI) adsorbed by dried *Bacillus cereus*.

compete with Cr(VI) ions for the adsorption sites on the surface of dried *Bacillus cereus*. The decrease of the biosorption efficiency when pH was beyond 2.95 might be attributed to the reduction of $H^+$ concentration and the formation of anionic hydroxide complexes which decreased the dissolved metal concentration in solution, and their competition with the active sites, which led to decreased Cr(VI) uptake (Ibrahim 2011).

### Effect of initial concentration of Cr(VI)

The combined effects of initial Cr(VI) concentration with pH and biosorbent dosage are shown in Figure 2(b) and (c). Because a driving force provided by the initial concentration of metal ions could overcome mass transfer resistance between the biosorbent and the biosorption medium, a higher initial metal concentration would have a beneficial effect on the dried *Bacillus cereus* sorption capacity. Such an effect was clearly shown in Figure 2(b) and (c): the adsorbed Cr(VI) amount rapidly increased with initial Cr(VI) concentration increasing from 100 to 165.30 mg $L^{-1}$, and roughly reached a maximum at 165.30 mg $L^{-1}$. However, when the initial ion concentration continued to increase, the metal uptake reached equilibrium and all sites were almost saturated with metals. Hence, the rate of increment of adsorption capacity gradually became slower.

### Confirmation experiments

The objective of the experimental design was to optimize the conditions to maximize the adsorbed Cr(VI) amount. On the basis of RSM, the optimum levels of factors for adsorbed Cr(VI) amount were 165.30 mg $L^{-1}$, 2.96, and 3.01 g $L^{-1}$ for initial Cr(VI) concentration, pH, and biosorbent dosage, respectively. Under the optimum conditions, the adsorbed amount was 30.93 mg $g^{-1}$ and the corresponding removal efficiency of Cr(VI) was 59.28%. Furthermore, to support the optimized data as given by numerical modeling under optimized conditions, confirmatory experiments were conducted with the parameters attained by the model, and the removal efficiency for Cr(VI) was found to be 31.34 mg $g^{-1}$. Based on these results, it could be said that the dried *Bacillus cereus* could be used for the removal of Cr(VI) from wastewater.

### Adsorption kinetics study

In order to understand sorption kinetics of Cr(VI) by dried *Bacillus cereus*, the pseudo-first- and second-order kinetics models were applied to experimental data. As shown in Figure 3(a), the adsorption rate was very rapid within the first 10 min, and the adsorption process was basically completed and reached equilibrium after 15 min. This probably
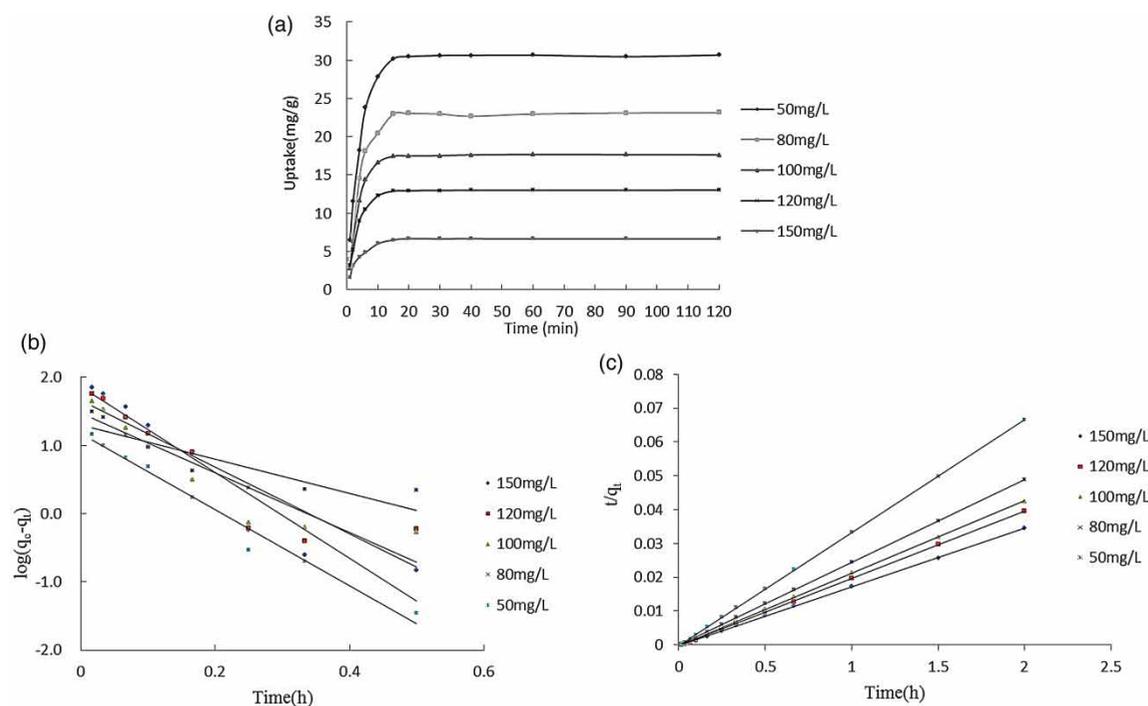


**Figure 3** │ Cr(VI) adsorption isotherms of dried *Bacillus cereus*: (a) at different initial Cr(VI) concentration; (b) Langmuir isotherm; (c) Freundlich isotherm.

reflects instantaneous adsorption or external surface adsorption, as previously reported (Han *et al.* 2010).

The parameters of both kinetic models and $R^2$ values are shown in Table 5. Figure 3(c) clearly indicates that the pseudo-second-order model gave a better prediction of the equilibrium uptake values for all initial Cr(VI) concentrations, and the correlation coefficients of pseudo-second-order kinetics were above 0.999 for all initial concentrations of Cr(VI).

## Adsorption isotherm models

In order to further investigate the biosorption mechanism of Cr(VI), the biosorption isotherm models (Langmuir and Freundlich) were used to characterize the interaction of concentrations of metal ions in solution ($C_e$; mg L$^{-1}$) with the amount of adsorbed metal ions on adsorbent ($q_e$; mg·g$^{-1}$) at equilibrium. Adsorption equation parameters were obtained from experimental data by using Equations (5) and (6). The results and correlation coefficients are presented in Figure 4 and Table 6. By comparing the constants and correlation coefficients $R^2$ (Table 1), it can be seen that the Langmuir model was more suitable for the experimental equilibrium sorption data than the Freundlich model. In this situation, the $R_L$ value was calculated as

0.0025 for Cr(VI) adsorption onto dried *Bacillus cereus*. So the adsorption of Cr(VI) ion onto dried *Bacillus cereus* was favorable.

## SEM analysis

Figure 5 shows the SEM images of dried *Bacillus cereus* biomass before and after Cr(VI) biosorption process at a magnification of 30,000. It is observed that the surface morphology of the biomass changed obviously after metal adsorption. Before Cr(VI) biosorption (Figure 5(a)), the material had a fluffy surface texture, and a highly irregular surface format was observed, which increased the contact area and favored sorption. SEM micrographs of the Cr(VI)-loaded biosorbent (Figure 5(b)) show a surface that is less fluffy and porous. This may be due to the adsorption of Cr(VI) on the outer surface of dried *Bacillus cereus* biomass, making the surface of dried *Bacillus cereus* biomass less fluffy and porous than its original form.

## Infrared spectroscopy study

As shown in Figure 6, the spectrum of unloaded biomass shows a broad absorption peak at 3,288 cm$^{-1}$, corresponding to the overlapping of −OH and −NH peaks (Gao *et al.* 2010). A peak at about 2,922 cm$^{-1}$ is assigned to the stretching vibrations of C–H bond of methylene groups. The peak at about 1,654 cm$^{-1}$ is caused by the stretching band of carboxyl groups. The weak band at 1,540 cm$^{-1}$ could be due to a combination of the stretching vibration of C–N and deformation vibration of N–H peptidic bond of protein (Amide II) (Gao *et al.* 2011). The weak peaks in the region of wave numbers 1,400–1,460 cm$^{-1}$ are representative of amino substituted alkyl groups. Besides, the weak band at 1,246 cm$^{-1}$ indicates the presence of carboxylic acids (Yadav 2005). The band at 1,062 cm$^{-1}$ could be

**Table 5** │ Kinetic parameters for the removal of Cr(VI) by dried *Bacillus cereus*

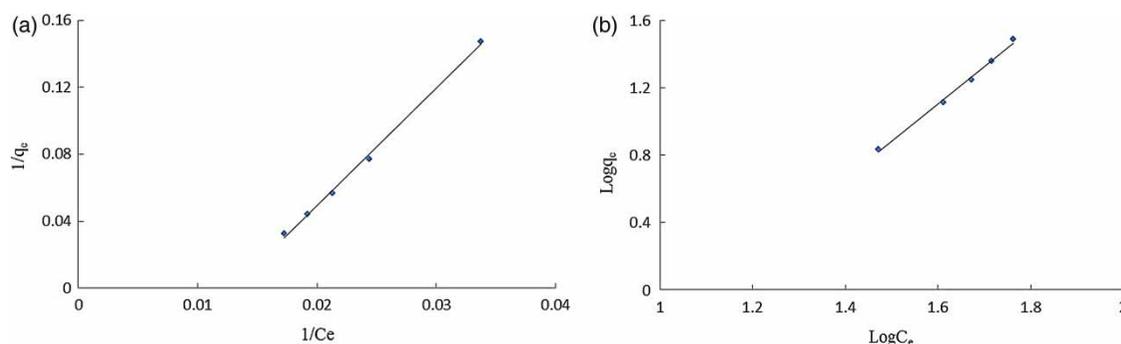|  | Pseudo-first-order kinetic model | Pseudo-second-order kinetic model |
|---|---|---|
| 150 mg L$^{-1}$ | 0.9215 | 0.998 |
| 120 mg L$^{-1}$ | 0.8261 | 0.999 |
| 100 mg L$^{-1}$ | 0.8494 | 0.998 |
| 80 mg L$^{-1}$ | 0.7842 | 0.999 |
| 50 mg L$^{-1}$ | 0.9785 | 0.999 |



**Figure 4** │ Plot of (a) pseudo-first-order kinetic equation and (b) second-order kinetic equation.

**Table 6** │ Langmuir and Freundlich adsorption model constants for Cr(VI) adsorption

| Model | $q_{max}$ (mg g$^{-1}$) | b (L mg$^{-1}$) | $R_L$ | $K_f$ | 1/n | $R^2$ |
|---|---|---|---|---|---|---|
| Langmuir | 30.01 | 7.0226 | 0.0025 | – | – | 0.9975 |
| Freundlich | | | | 0.0035 | 2.2213 | 0.9948 |
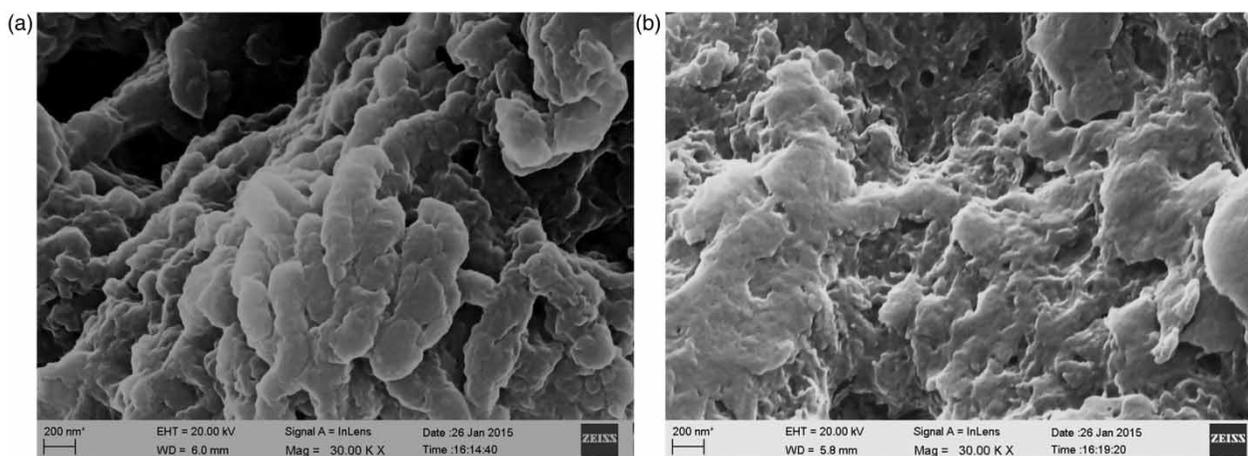


**Figure 5** │ The SEM micrograph of dried *Bacillus cereus* before (a) and after (b) Cr(VI) adsorption.
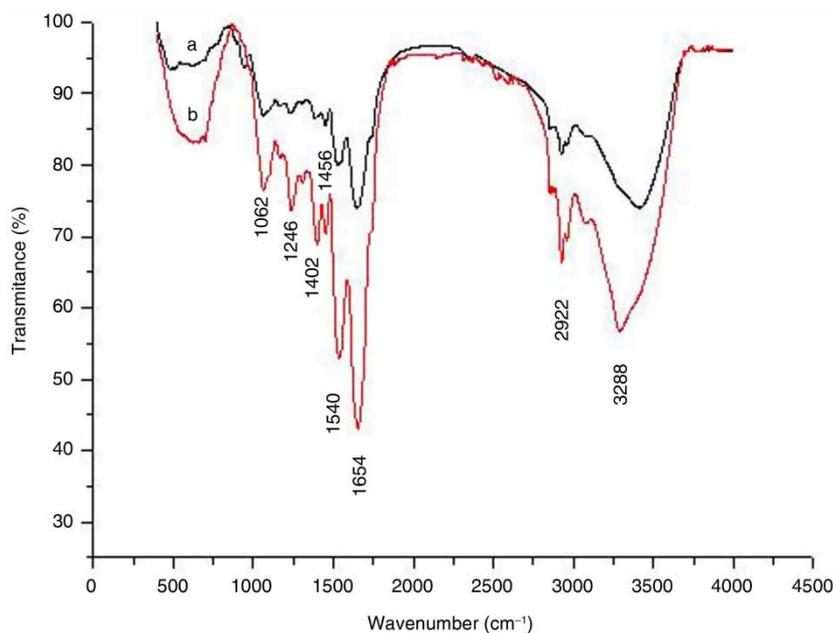


**Figure 6** │ FTIR spectra of unloaded (a) and Cr(VI)-loaded (b) dried *Bacillus cereus*.

attributed to the stretching vibration of O–H of polysaccharides. Meanwhile, some bands in the fingerprint region could be related to the phosphate groups. After Cr(VI) was loaded, a change of peak positions was observed at 1,062, 1,242, 1,400, 1,456, 1,539, 1,654 , 2,923 and 3,288 cm$^{-1}$. The significant changes in the wave number of these peaks after loading of Cr(VI) indicated that the functional groups (C–N, N–H, carboxyl groups, C–H, hydroxyl and O–H) were

involved in the biosorption of Cr(VI) on the surface of dried *Bacillus cereus*.

## CONCLUSION

To optimize the Cr(VI) biosorption by the dried *Bacillus cereus*, RSM was used to study the combined and individual effects of operating parameters (pH, biomass dosage, and initial Cr(VI) concentration) on Cr(VI) adsorption capacity. The experimental results showed the effect of biosorbent dosage was the most significant. The second-order polynomial equation model whose validity was agreed upon was estimated which was suitable for the experimental data. The optimum adsorption conditions for removal of Cr(VI) were 165.30 mg L$^{-1}$, 2.96, and 3.01 g L$^{-1}$ for initial Cr(VI) concentration, pH, and biosorbent dosage, respectively. Under these conditions, maximum adsorbed amount and removal efficiency of Cr(VI) were 30.93 mg g$^{-1}$ and 59.28%, respectively. This study also revealed that the Langmuir isotherm was more suitable than the Freundlich isotherm for biosorption by dried *Bacillus cereus*, and the kinetics of Cr(VI) adsorption followed the pseudo-second-order rate equation. Based on the above experiments, it could be concluded that RSM was a powerful statistical method for optimization of experimental conditions, and dried *Bacillus cereus* as an eco-friendly biosorbent showed a remarkable performance in the removal of Cr(VI).

## ACKNOWLEDGEMENTS

## REFERENCES

Al-Rub, F. A. A., El-Naas, M. H., Ashour, I. & Al-Marzouqi, M. 2006 Biosorption of copper on *Chlorella vulgaris* from single, binary and ternary metal aqueous solutions. *Process Biochemistry* **41** (2), 457–464.

Amini, M., Younesi, H., Bahramifar, N., Lorestani, A. A. Z., Ghorbani, F., Daneshi, A. & Sharifzadeh, M. 2008 Application of response surface methodology for optimization of lead biosorption in an aqueous solution by *Aspergillus niger*. *Journal of Hazardous Materials* **154** (1–3), 694–702.

Amini, M., Younesi, H. & Bahramifar, N. 2009 Biosorption of nickel(II) from aqueous solution by *Aspergillus niger*: response surface methodology and isotherm study. *Chemosphere* **75** (11), 1483–1491.

Buntić, A., Pavlović, M., Mihajlovski, K., Randjelović, M., Rajić, N., Antonović, D., Šiler-Marinković, S. & Dimitrijević-Branković, S. 2013 Removal of a cationic dye from aqueous solution by microwave activated Clinoptilolite – response surface methodology approach. *Water, Air, & Soil Pollution* **225** (1), 1–13.

Çelekli, A. & Bozkurt, H. 2011 Bio-sorption of cadmium and nickel ions using *Spirulina platensis*: kinetic and equilibrium studies. *Desalination* **275** (1–3), 141–147.

Choppala, G., Bolan, N. & Park, J. H. 2013 Chapter two – chromium contamination and its risk management in complex environmental settings. *Advances in Agronomy* **120**, 129–172.

Das, N. 2010 Recovery of precious metals through biosorption – a review. *Hydrometallurgy* **103** (1–4), 180–189.

Demirbas, A. 2008 Heavy metal adsorption onto agro-based waste materials: a review. *Journal of Hazardous Materials* **157** (2–3), 220–229.

Flouty, R. & Estephane, G. 2012 Bioaccumulation and biosorption of copper and lead by a unicellular algae *Chlamydomonas reinhardtii* in single and binary metal systems: a comparative study. *Journal of Environmental Management* **111**, 106–114.

Gao, J., Zhang, Q., Su, K., Chen, R. & Peng, Y. 2010 Biosorption of acid yellow 17 from aqueous solution by non-living aerobic granular sludge. *Journal of Hazardous Materials* **174** (1–3), 215–225.

Gao, J., Zhang, Q., Wang, J., Wu, X., Wang, S. & Peng, Y. 2011 Contributions of functional groups and extracellular polymeric substances on the biosorption of dyes by aerobic granules. *Bioresource Technology* **102** (2), 805–813.

Güzel, F., Sayğılı, H., Akkaya Sayğılı, G. & Koyuncu, F. 2015 New low-cost nanoporous carbonaceous adsorbent developed from carob (*Ceratonia siliqua*) processing industry waste for the adsorption of anionic textile dye: characterization, equilibrium and kinetic modeling. *Journal of Molecular Liquids* **206** (0), 244–255.

Han, R., Wang, Y., Sun, Q., Wang, L., Song, J., He, X. & Dou, C. 2010 Malachite green adsorption onto natural zeolite and reuse by microwave irradiation. *Journal of Hazardous Materials* **175** (1–3), 1056–1061.

Ibrahim, W. M. 2011 Biosorption of heavy metal ions from aqueous solution by red macroalgae. *Journal of Hazardous Materials* **192** (3), 1827–1835.

Landaburu-Aguirre, J., Pongrácz, E., Perämäki, P. & Keiski, R. L. 2010 Micellar-enhanced ultrafiltration for the removal of cadmium and zinc: use of response surface methodology to improve understanding of process performance and optimisation. *Journal of Hazardous Materials* **180** (1–3), 524–534.

Li, X., Liu, S., Na, Z., Lu, D. & Liu, Z. 2013 Adsorption, concentration, and recovery of aqueous heavy metal ions

with the root powder of *Eichhornia crassipes*. *Ecological Engineering* **601**, 160–166.

Ngah, W. S. W. & Hanafiah, M. A. K. M. 2008 Removal of heavy metal ions from wastewater by chemically modified plant wastes as adsorbents: a review. *Bioresource Technology* **99** (10), 3935–3948.

Rubio, J., Souza, M. L. & Smith, R. W. 2002 Overview of flotation as a wastewater treatment technique. *Minerals Engineering* **15** (3), 139–155.

Şahan, T. & Öztürk, D. 2014 Investigation of Pb(II) adsorption onto pumice samples: application of optimization method based on fractional factorial design and response surface methodology. *Clean Technologies and Environmental Policy* **16** (5), 819–831.

Saraswat, S. & Rai, J. P. N. 2010 Heavy metal adsorption from aqueous solution using *Eichhornia crassipes* dead biomass. *International Journal of Mineral Processing* **94** (3–4), 203–206.

Sarkar, M. & Santra, D. 2015 Modeling fluoride adsorption on cerium-loaded cellulose bead – response surface methodology, equilibrium, and kinetic studies. *Water, Air, & Soil Pollution* **226** (3), 1–14.

Suazo-Madrid, A., Morales-Barrera, L., Aranda-García, E. & Cristiani-Urbina, E. 2011 Nickel(II) biosorption by *Rhodotorula glutinis*. *Journal of Industrial Microbiology & Biotechnology* **38** (1), 51–64.

Subbaiah, M. & Yun, Y. 2013 Biosorption of nickel(II) from aqueous solution by the fungal mat of *Trametes versicolor* (rainbow) biomass: equilibrium, kinetics, and thermodynamic studies. *Biotechnology and Bioprocess Engineering* **18** (2), 280–288.

Turkyilmaz, H., Kartal, T. & Yildiz, S. Y. 2014 Optimization of lead adsorption of mordenite by response surface methodology: characterization and modification. *Journal of Environmental Health Science and Engineering.* doi: 10.1186/2052-336x-12-5.

Wang, J. & Chen, C. 2009 Biosorbents for heavy metals removal and their future. *Biotechnology Advances* **27** (2), 195–226.

Yadav, L. D. S. 2005 *Introduction to Spectroscopy (Spectrometry)*. Springer, The Netherlands, pp. 1–6.